

Molecular dynamics simulation study of friction and diffusion of a tracer in a Lennard–Jones solvent

Song Hi Lee

Received: 18 February 2010/Accepted: 8 April 2010/Published online: 4 May 2010
© Springer-Verlag 2010

Abstract The friction and diffusion coefficients of a tracer in a Lennard–Jones (LJ) solvent are evaluated by equilibrium molecular dynamics simulations in a micro-canonical ensemble. The solvent molecules interact through a repulsive LJ force each other and the tracer of diameter σ_2 interacts with the solvent molecules through the same repulsive LJ force with a different LJ parameter σ . Positive deviation of the diffusion coefficient D of the tracer from a Stokes–Einstein behavior is observed and the plot of $1/D$ versus σ_2 shows a linear behavior. It is also observed that the friction coefficient ζ of the tracer varies linearly with σ_2 in accord with the prediction of the Stokes formula but shows a smaller slope than the Stokes prediction. When the values of ratios of sizes between the tracer and solvent molecules are higher than 5 approximately, the behavior of the friction and diffusion coefficients is well described by the Einstein relation $D = k_B T / \zeta$, from which the tracer is considered as a Brownian particle.

Keywords Friction · Diffusion · Tracer · Lennard–Jones solvent · Molecular dynamics simulation · Brownian particle · Stoke-Einstein formula

1 Introduction

Understanding friction and diffusion properties of molecules in liquids is a fundamental problem in statistical mechanics and the physics of liquid state. They are important for basic and applied problems in physical

chemistry and biology since many processes are diffusion limited. Most of the mixtures and solutions of these two domains are characterized by very large size and mass ratios between the solute and solvent molecules. In colloids and micellar solutions, the large and massive particles such as micelles or colloids which coexist with the atoms, ions, or small molecules of the solvent are typical examples of so-called Brownian particles.

It is well known that the diffusion coefficient D of a large and massive particle immersed in a solvent of much smaller and lighter particles is related to the solvent viscosity η by the Stokes–Einstein (SE) equation

$$D = \frac{k_B T}{C \pi \eta r_2} \quad (1)$$

where T is the absolute temperature, k_B the Boltzmann constant, and r_2 the radius of the diffusing particle. C is the hydrodynamic boundary condition which is 4 for ‘slip’ and 6 for ‘stick’ [1]. This relation has been verified experimentally in great detail [2] and is theoretically well understood [3]. If the size of the diffusing particle is not large compared to that of the solvent molecule, the Stokes–Einstein relation is not expected to remain valid.

When the tracers have a quasi-macroscopic size, from hydrodynamic arguments the Stokes law can be derived. It gives an expression of the friction coefficient

$$\zeta = C \pi \eta r_2. \quad (2)$$

In many suspensions, the values of ratios of masses and sizes between the solute and solvent molecules are only the order of 10 and the possibility that the solute can be considered as a Brownian particle becomes questionable. The problem here is that of the determination of the lower bounds of the size and mass ratios above which the motion of the solute is Brownian. The criterion chosen to locate

S. H. Lee (✉)
Department of Chemistry, Kyungsung University,
Busan 608-736, South Korea
e-mail: shlee@ks.ac.kr

these bounds is that the diffusion coefficient of the solute obeys the Einstein relation between D and ζ :

$$D = \frac{k_B T}{\zeta}. \quad (3)$$

Ould-Kaddour and Levesque performed a molecular dynamics (MD) to determine the range of the size and mass values of the solute particles where the solute diffusion coefficient is well estimated from the SE formula. They concluded that positive deviations from the SE formula are observed as the size ratio or the mass ratio of the tracer to the solvent molecules is lowered and that for equal solvent and tracer molecular masses, the crossover to the hydrodynamics regimes is found to occur when the size ratio is ~ 4 [4].

Willeke [5] also carried out MD simulations to investigate the mass ratio dependence of the tracer self-diffusion coefficient as a function of density and length diameter ratio σ_{22}/σ_{11} and found that for $\sigma_{22}/\sigma_{11} > 1$ the SE prediction is not valid for mass ratios $1/16 \leq m_2/m_1 \leq 50$, and for $\sigma_{22}/\sigma_{11} > 2$ and for $m_2/m_1 < 1$ the SE regime is reached for smaller densities than for the same system but $m_2/m_1 > 1$.

The test of SE formula for the size ratio or the mass ratio of the tracer was further discussed by Sokolovskii et al. [6] for hard sphere fluids, by Cappelezzo et al. [7] for Lennard-Jones (LJ) fluids, by Funazukuri et al. [8] for supercritical and liquid conditions, and by Harris [9] for LJ, molecular, and ionic liquids.

In a recent study [10], the friction and diffusion coefficients of a massive Brownian particle in a mesoscopic solvent are computed from the force and the velocity autocorrelation functions. There are no intermolecular forces among the solvent molecules. The mesoscopic solvent is described in terms of free streaming of the solvent molecules, interrupted at discrete time intervals by multiparticle collisions[11–13] that conserve mass, momentum, and energy, and the Brownian particle interacts with the solvent molecules through repulsive Lennard-Jones forces. The friction coefficient can be determined accurately from either the decay rate of the momentum autocorrelation function or the extrapolation of the long time decay of the force autocorrelation function to $t = 0$, provided the number N of solvent molecules is sufficiently large, typically $N > 30,000$. Hydrodynamics effects on the velocity autocorrelation function and diffusion coefficient are studied as a function of Brownian particle mass and diameter.

The purpose of this paper is twofold: First, we investigate to locate the lower bounds of the size ratio above which the motion of the solute is Brownian according to the criterion that the diffusion coefficient of the solute obeys the Einstein relation, Eq. 3, by carrying out simple

molecular dynamics (MD) simulations of a tracer in a LJ solvent. Second, we use these calculations to predict friction and diffusion properties of the LJ particle as functions of the size and mass ratios, especially for anti-Brownian particle which has a small size and light mass compared to those of the solvent molecule. This paper is organized as follows: We present briefs of molecular models and MD simulation methods in next section, theories for friction and diffusion properties in Sect. 3, our simulation results in Sect. 4 and concluding remarks in Sect. 5.

2 Molecular models and NVT MD simulations

It is often useful to divide more realistic potentials into separate attractive and repulsive components, and the separation proposed by Weeks et al. [14] involves splitting the potential at the minimum (r_m). For the Lennar-Jones (LJ) potential, the repulsive part is called the WCA potential:

$$v^{\text{WCA}}(r) = \begin{cases} 4\varepsilon \left[\left(\frac{\sigma}{r}\right)^{12} - \left(\frac{\sigma}{r}\right)^6 \right] + \varepsilon, & r \leq r_m = 2^{1/6}\sigma \\ 0, & r \geq r_m \end{cases} \quad (4)$$

It should be noted that the potential $v^{\text{WCA}}(r)$ is significantly harder than the inverse 12th power soft-sphere potential, which is sometimes thought of as the repulsive part of $v^{\text{LJ}}(r)$. The LJ parameters for the solvent molecules are chosen as $\sigma_2 = \sigma_1 = 0.2$ nm and $\varepsilon = \varepsilon_1 = 1.00604$ kJ/mol. The preliminary microcanonical ensemble (NVE fixed) molecular dynamics (MD) simulation for $N = 32,000$ LJ particles of mass of $m = 3.9948$ g/mol was started in the cubic box of length $L = 6.84$ nm, of which the density is equal to 0.66334 g/cm³. The corresponding reduced number density is $\rho^* = \rho\sigma_1^3 = (N/V)\sigma_1^3 = 0.8$ which is a typical value used for several MD simulation studies for transport coefficients of the LJ model fluid [15]. The temperature of the system is chosen as 40.33 K for comparison with the mesoscopic solvent case [10] and $T^* = k_B T / \varepsilon_1 = 1/3$.

After a full equilibration of the solvent-only system, a Lennard-Jones particle with various size (σ_2) and mass (M) is introduced at the center of the cubic simulation box. The tracer and LJ solvent molecule interacts through the above WCA potential with LJ parameters of $\sigma = (\sigma_1 + \sigma_2)/2$ and the same $\varepsilon = \varepsilon_1 = \varepsilon_2$. In the beginning of each MD simulation, the value of σ_2 is increased gradually from zero to σ_2 . Three set of M and σ_2 are chosen. (1) $\sigma_2 = \sigma_1$ and $M/m = 0.1, 0.5, 1, 5, 20$, and 100 , (2) $M = m$ and $\sigma_2/\sigma_1 = 0.02, 0.1, 0.5, 1, 2, 5$, and 10 , and (3) $M = \infty$ and $\sigma_2/\sigma_1 = 0.02, 0.1, 0.5, 1, 2, 5$, and 10 . For size ratios higher than 1, in order to maintain a constant value of the pressure, the volume of the box was slightly increased by

an amount that corresponds the excess volume occupied by the tracer and so the length of the cubic simulation box for the system is redefined by $(N/L^3)\sigma_1^3 + (1/L^3)\sigma_2^3 = 0.8$.

Long range corrections to the energy, pressure, etc. due to the potential truncation were included in these properties by assuming that the pair distribution function was uniform beyond the cutoff distance [16]. The equations of motion were solved using the velocity Verlet algorithm [17] with a time step of 0.2×10^{-14} s. The systems were fully equilibrated and the equilibrium properties were averaged over four blocks of 1,000,000 time steps of 10 different initial configurations. The configurations of LJ particles were stored every five time steps for further analysis.

3 Transport coefficients and time-dependent autocorrelation functions

Shear viscosity of the LJ solvent is calculated by the modified Green–Kubo formula for better statistical accuracy [18]:

$$\eta = \frac{V}{k_B T} \int_0^\infty dt \sum_i \langle P_{i\alpha\beta}(t) \cdot P_{i\alpha\beta}(0) \rangle, \quad (5)$$

where

$$P_{i\alpha\beta} = \frac{1}{V} \left[mv_{i\alpha}(t) \cdot v_{i\beta}(t) + \sum_{j \neq i} r_{i\alpha}(t) \cdot f_{j\beta}(t) \right] \quad (6)$$

with $\alpha\beta = xy, xz, yx, yz, zx$, and zy , and diffusion coefficient of the tracer is obtained through the Einstein formula from mean square displacements (MSD):

$$D = \frac{1}{6} \lim_{t \rightarrow \infty} \frac{d\langle |r(t) - r(0)|^2 \rangle}{dt}. \quad (7)$$

Transport properties are typically determined in molecular dynamics (MD) simulations in the microcanonical ensemble and some subtle issues are encountered when determining the friction coefficient from such simulations. These issues have been discussed by Espanol and Zuniga [19]. Briefly, they are as follows: A time dependent friction coefficient $\zeta_u(t)$ in terms of the force autocorrelation function is defined,

$$\zeta_u(t) = \frac{1}{3k_B T} \int_0^t d\tau \lim_{M \rightarrow \infty} \langle \mathbf{F}(\tau) \cdot \mathbf{F}(0) \rangle \quad (8)$$

and through the Laplace transforms of the projected and unprojected force autocorrelation functions [20–22], in space, the following relation is obtained

$$\zeta_u(t) = \zeta e^{-\zeta t/\mu}. \quad (9)$$

The friction coefficient may then be estimated from the extrapolation of the long time decay of the force autocorrelation function $\zeta_u(t)$ to $t = 0$ or from the decay rates of $\zeta_u(t)$.

The momentum autocorrelation function can be determined from the Langevin equation and decays exponentially as

$$C(t) = \langle \mathbf{P}(t) \cdot \mathbf{P}(0) \rangle / \langle P(0)^2 \rangle = e^{-\zeta t/\mu}. \quad (10)$$

The friction coefficient can be determined from the long time decay rate of the momentum autocorrelation function.

In the microcanonical ensemble $\langle P^2 \rangle = 3k_B T \mu = 3k_B T M N m / (M + N m)$ [19]. If the limit $M \rightarrow \infty$ is first taken in the calculation of the time dependent friction coefficient, then $\mu = N m$. Since MD simulations are carried out at finite N , the study of the N (and M) dependence of $\zeta_u(t)$ and the estimate of the friction coefficient from either the decay of the momentum or force correlation functions is of interest. This has prompted the MD simulations of the momentum and force autocorrelation functions as a function of N into explore this question [10, 19, 23].

It is most interesting that for long times the values of $\zeta_u(t)$ can be obtained by the time derivative of $C(t)$ in Eq. 10:

$$\begin{aligned} -Nm \frac{d}{dt} C(t) &= \frac{1}{3k_B T} \langle \mathbf{F}(t) \cdot \mathbf{P}(0) \rangle \\ &= \frac{1}{3k_B T} \lim_{s \rightarrow \infty} \frac{1}{s} \int_0^s du \mathbf{F}(u+t) \cdot \mathbf{P}(u) \\ &= -\frac{1}{3k_B T} \lim_{s \rightarrow \infty} \frac{1}{s} \int_0^s du \mathbf{F}(u) \cdot \mathbf{P}(u+t) \\ &= \frac{1}{3k_B T} \lim_{s \rightarrow \infty} \frac{1}{s} \int_0^s d\tau \mathbf{F}(\tau) \cdot \mathbf{P}(u+\tau) \\ &= -\frac{1}{3k_B T} \int_0^t d\tau \mathbf{F}(\tau) \cdot \mathbf{P}(0) = \xi_u(t), \end{aligned} \quad (11)$$

where $\langle P^2 \rangle = 3k_B T M N m$ and $\mathbf{P}(t) = - \int_0^t d\tau \mathbf{F}(\tau)$ were used, and vice versa:

$$1 - \frac{1}{Nm} \int_0^t d\tau \zeta(\tau) = c(t), \quad (12)$$

where $\zeta_u(t)$ and $c(t)$ are used to distinguish from $\zeta_u(t)$ and $C(t)$ in Eqs. 9 and 10, respectively. Substitution of $C(t)$ in Eq. 10 into Eq. 11 recovers Eq. 9 and also Eq. 10 is recovered by substitution of $\zeta_u(t)$ in Eq. 9 into Eq. 12.

4 Results and discussion

The viscosity for the solvent-only system of $N = 32,000$ Lennard–Jones (LJ) particles of mass $m = 3.995$ g/mol in

the cubic simulation box of length $L = 6.84$ nm interacting through the WCA potential with LJ parameters $\sigma = 0.2$ nm and $\varepsilon = 1.00604$ kJ/mol at $T = 40.33$ K obtained from Eq. 5 is $\eta = 2.53 \pm 0.02$ mP (10^{-4} kg/m·s) and the reduced viscosity $\eta^* = \eta\sigma^2(m)^{1/2} = 12.2$.

For the case of $\sigma_2 = \sigma_1 = 0.2$ nm and $M/m = 0.1, 0.5, 1, 5, 20$, and 100, the diffusion coefficient of the tracer is estimated as a function of M/m and is plotted in Fig. 1. The prediction from the Stokes–Einstein (SE) Eq. 1 is that D should be independent of M/m . This prediction is borne out for $\sigma_2/\sigma_1 = 1$ (intra-diffusion): however, from our MD simulations we found that D seems decreasing with increasing M/m for mass ratios M/m between 0.1 and 5. Using the SE relation with the slip boundary condition would yield an underestimate of D and positive deviation from the SE relation appears over the whole range of M/m . In Fig. 1 the dotted line indicates the value of D_{SE} at $\sigma_2/\sigma_1 = 0.1$. We also observed that the hydrodynamics limit, i.e., mass independent behavior, is reached for M/m above 5. That is, D first decreases as the tracer mass increases, and then levels off at a mass independent value. This leveling-off takes place for mass ratios M/m between 5 and 100.

In Fig. 2 we plot the diffusion coefficient of the tracer as a function of σ_2/σ_1 for the case of mass ratio equal to 1. In order to facilitate the comparison with the SE relation, we plot $1/D$ as a function of σ_2/σ_1 in Fig. 1. $1/D$ increases first quadratically and then almost linearly as the size ratio increases. Hence, the behavior of $1/D$ versus σ_2/σ_1 is essentially linear for σ_2/σ_1 higher than 2 and that of $1/D_{SE}$ predicted from the Stokes–Einstein relation with the slip boundary condition is also linear, of course, but for all the range of σ_2/σ_1 , D_{SE} slightly underestimates the diffusion coefficient of the tracer. For example, the ratio of the diffusion coefficient as obtained from our molecular dynamics (MD) simulations to that given by the SE relation is

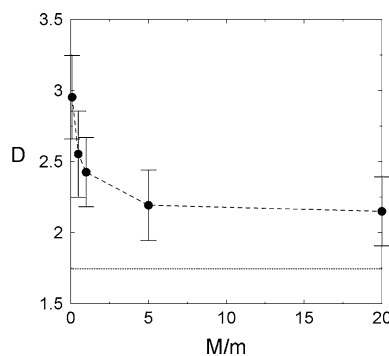


Fig. 1 Diffusion coefficient, D ($10^{-5}\text{cm}^2/\text{s}$), of the tracer as a function of M/m (the point of $D = 1.943 \times 10^{-5}\text{cm}^2/\text{s}$ at $M/m = 100$ is omitted). The dotted line indicates the value of D_{SE} ($= 1.75 \times 10^{-5}\text{cm}^2/\text{s}$) at $\sigma_2/\sigma_1 = 1.0$

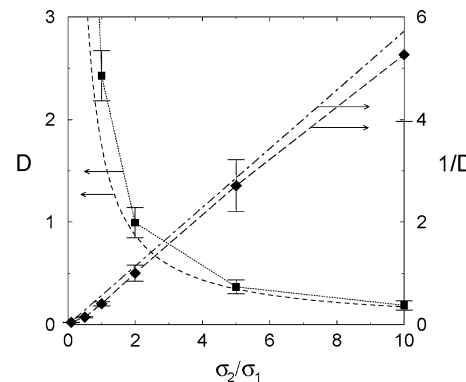


Fig. 2 Diffusion coefficient, D ($10^{-5}\text{cm}^2/\text{s}$), of the tracer as a function of σ_2/σ_1 : filled square D_{MD} as a function of σ_2/σ_1 ; filled diamond $1/D_{MD}$ as a function of σ_2/σ_1 ; dashed line, $D_{SE}=k_B T/4\pi\eta r_2$ as a function of σ_2/σ_1 ; and dot-dashed line, $1/D_{SE}$ as a function of σ_2/σ_1

$D_{MD}/D_{SE} = 1.14, 1.06$, and 1.09 for $\sigma_2/\sigma_1 = 2, 5$, and 10 , respectively.

In the definition of the friction coefficient three limit procedures are involved; the long time limit ($t \rightarrow \infty$); the thermodynamic limit ($N \rightarrow \infty$); and the infinite mass limit $M \rightarrow \infty$ [19]. The Langevin approximation is expected to be valid for a finite but sufficiently large mass of the tracer and for a large number of solvent particles. If we first consider the infinite time limit the resulting friction coefficient is zero. The only way to have a non-zero value for the friction coefficient is by first taking $M \rightarrow \infty$. In the thermodynamic limit $N \rightarrow \infty$, the projected and unprojected force autocorrelation functions are the same [10, 20–22] and the expression Eq. 8 is possible. Since MD simulations are carried out at finite N , the study of the N (and M) dependence of $\zeta_u(t)$ and the estimate of the friction coefficient from either the decay of the momentum or force autocorrelation functions is of interest.[10, 23]

In order to calculate the friction coefficients of the tracer from Eqs. 8 and 10, the mass of the tracer, M , becomes infinity, or the tracer is fixed in space using a holonomic constraint method [24]. While the MD simulation by using an infinite mass violates the equation of motion since the tracer never moves with the force on it, the constraint method MD simulation returns the tracer back to its original position with zero velocity, and trajectories by both MD simulations are not the same. However, it is found that the momentum of the whole system carried out by both the infinite mass and the constraint method MD simulations are not conserved, because the momentum of the tracer is not well defined with zero velocity and infinite mass. Nevertheless, the momentum of the fixed particle is defined as the negative of the total momentum of the solvent particles [19, 23]. A reasonable trick for this difficulty is to put the mass of the tracer as 10^{90} g/mol, and in this case the

momentum of the system is conserved: the magnitude of the mass of the tracer is on the order of 90 and its velocity is on the order of −90, but its momentum has a finite value and is equal to the negative of the total momentum of the solvent particles.

In Fig. 3 we plot the logarithm of the time dependent friction coefficients $\zeta_u(t)$ and $\xi_u(t)$, and that of the momentum autocorrelation functions $C(t)$ and $c(t)$ for the system of $\sigma_2 = 2.0, obtained from the momentum-conserved MD simulations. A total of 6 friction coefficients are estimated from these quantities. The first two, ζ_1 and ζ_2 , can be obtained directly from $\zeta_u(t)$, from the extrapolation of the exponential long time-decay of $\zeta_u(t)$ to $t = 0$ ζ_2 and from the decay rate of $\zeta_u(t)$ (ζ_2), according to Eq. 9. We have found that ζ_1 may be determined correctly [10, 25] and the final value of ζ_1 obtained from Fig. 3 is 1.25 kg/(mol·ps). However, it is difficult to determine ζ_2 from the slope of $\zeta_u(t)$, $-\zeta_2/Nm$, especially for very large N where the slope is close to zero. While the slopes scale as $1/N$ for the smaller N values, the small value of the slope and relatively large statistical error makes it difficult to determine this scaling for very large values of N .$

The third is obtained from the decay rate, $-\zeta_3/Nm$, of the normalized autocorrelation function, $C(t)$. The momentum autocorrelation functions of the tracer calculated from three different MD simulations are wrong (not shown). The main problem is the momentum conservation of the system. In the case of the momentum-conserved MD simulation, the total instantaneous momentum of the whole system is on the order of $-5 \sim -6$, even when using the double precision code. This might be related to the well-known rounding error in calculation of velocity in the usual MD simulation.

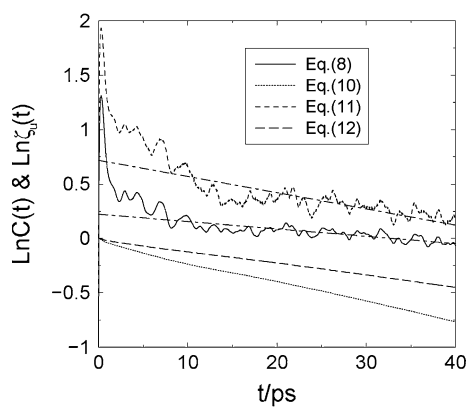


Fig. 3 Logarithms of the time dependent friction coefficients and normalized momentum autocorrelation functions for the case of $\sigma_2 = 2.0\text{ nm}$. Solid line, $\zeta_u(t)$ calculated directly from Eq. 8; dotted line, $C(t)$ calculated directly from Eq. 10; dashed line, $\xi_u(t)$ obtained by the time differentiation of the dashed line $C(t)$ using Eq. 11; and long-dashed line, $c(t)$ obtained by the time integration of the dotted line $\zeta_u(t)$ using Eq. 12. The two straight dot-dashed lines are the extrapolation of the exponential long time-decay to $t = 0$ to determine ζ 's

The next possible explanation for this is related to the thermodynamic limit ($N \rightarrow \infty$). In our MD simulation, since $Nm = 127.84\text{ kg/mol}$, the slope of the logarithm of $C(t)$, $-\zeta_3/Nm$, should be -0.0098 ps to get ζ_3 as the same value of $\zeta_1 = 1.25\text{ kg}/(\text{mol}\cdot\text{ps})$ above, which means that, at $t = 40\text{ ps}$, $\ln C(t) = -0.39$ and $C(t) = 0.68$. Hence, the decay of $C(t)$ should be very small even after 40 ps. Since $-\zeta_3/Nm$ scales as N^{-1} , $C(t)$ should decay very slowly for large N . However, the actual value of $\ln C(t)$ at $t = 40\text{ ps}$ is -0.77 as seen in Fig. 3 and the final value of ζ_3 obtained from Fig. 3 is $2.29\text{ kg}/(\text{mol}\cdot\text{ps})$.

The fourth and fifth are obtained from $\xi_u(t)$, which is derived by the time differentiation of $C(t)$ using Eq. 11, like ζ_1 and ζ_2 , according to Eq. 9. It is notable that the behavior of $\xi_u(t)$ has a similarity to that of $\zeta_u(t)$ with a multiplying factor. However, these friction coefficients are wrong since $C(t)$ is incorrect. The final friction coefficient is obtained from the decay rate, $-\zeta_6/Nm$, of $c(t)$. Since $\zeta_u(t)$ calculated directly from Eq. 8 is correct, $c(t)$ obtained by the time integration of $\zeta_u(t)$ using Eq. 12 is also correct. As discussed for $C(t)$ above, $c(t)$ should also decay very slowly for large N and the value of $\ln c(t)$ at $t = 40\text{ ps}$ is -0.43 as seen in Fig. 3. The final value of ζ_6 obtained from Fig. 3 is $1.37\text{ kg}/(\text{mol}\cdot\text{ps})$. If the momentum autocorrelation function $C(t)$ calculated directly from Eq. 10 is correct, then $\xi_u(t)$ obtained by time differentiation of $C(t)$ using Eq. 11 should be the same as $\zeta_u(t)$ calculated directly from Eq. 8. That is, $C(t)$ is not small enough to encounter the factor Nm ($= 127.84\text{ kg/mol}$) in Eq. 11 for some reason. In order for $C(t)$ to be the same to $c(t)$, $C(t)$ should be reduced in proportion to the ratio of the slopes $\zeta_6/\zeta_3 = 1.37/2.29 = 0.60$ to encounter the factor Nm in Eq. 8.

In the previous mesoscopic molecular dynamics (MD) simulation study [10] the systems were such that $N = 5,120 \sim 327,680$, $M/m = 5$ $N \sim 200$ N and $M = \infty$. The obtained friction coefficients of the Brownian particle from $C(t)$ and $\zeta_u(t)$ were almost the same for various values of N and M , which means the calculated $C(t)$ were correct and the decay of $C(t)$ scaled very well as N^{-1} . $C(t)$ and $c(t)$, and $\zeta_u(t)$ and $\xi_u(t)$ for various values of N and M were difficult to distinguish in the figures. In this mesoscopic MD simulation using multiparticle collision dynamics, the system is divided into several cells in which the mass, momentum and energy are conserved. While the solvent particles only near the Brownian particle interact with it, the other particles far from the Brownian particle are momentum-conserved in each cell. Since the momentum of the Brownian particle is defined as the negative of the total momentum of the solvent particles, the decay of $C(t)$ is very slow for large N . In the present MD simulation study, the solvent particles interact with each other and the momentum of the solvent particles far from the tracer is in question. If we neglect the interaction between solvent particles, then

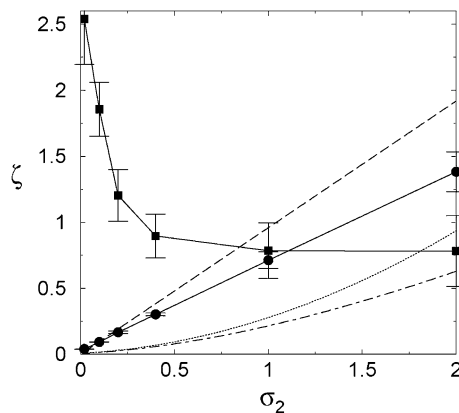


Fig. 4 Friction coefficient, ζ (kg/mol·ps), of the tracer and $\zeta D/k_B T$ as a function of σ_2 . filled circle ζ_{MD} ; filled square $\zeta_{MDDMD/k_B T}$; dotted line, $\zeta_m = 8/3\rho\sigma_{12}^2(2\pi mk_B T)^{1/2}$; dashed line, $\zeta_h = 4\pi\eta r_2$; and dot-dashed line, ζ_t

only short CWA interactions between the tracer and the near solvent particles exist, and the other particles far from the tracer undergo free streaming motion. In this case, we expect that the decay of $C(t)$ is very slow for large N . This test system is currently under study.

Figure 4 shows the friction coefficients obtained from our momentum-conserved MD simulations as a function of σ_2 . One sees that the friction coefficient varies linearly with σ_2 in accord with the prediction of the Stokes formula, Eq. 2. The hydrodynamic estimate of the friction $\zeta_h = C\pi\eta r_2$ versus σ_2 with the slip boundary condition ($C = 4$) using the independently computed viscosity $\eta = 2.53 \times 10^{-4}$ kg/m·s of the solvent-only system is also plotted in the same figure. The slopes are different from each other: 0.115×10^{-2} and 0.159×10^{-2} kg/m·s, respectively. If the hydrodynamic boundary condition is chosen as $C = 2.9$ instead of 4, the two lines coincide with each other. Therefore the slip boundary condition seems in the present work to hold better than the stick boundary condition, which is more expected for a repulsive LJ type interaction between solute and solvent molecules.

With a rough estimate of the microscopic contribution to the friction obtained using a hard sphere binary collision model with the collision diameter chosen to be $\sigma_{12} = (\sigma_1 + \sigma_2)/2$: $\zeta_m = 8/3\rho\sigma_{12}^2(2\pi mk_B T)^{1/2}$, an estimate of the friction that accounts for both microscopic and hydrodynamic contributions to the friction is given by $\zeta^{-1} = \zeta_m^{-1} + \zeta_h^{-1}$ [26]. The theoretical prediction (ζ_t) strongly underestimates our MD simulation result for all the values of σ_2 . Comparing with the previous mesoscopic MD simulation study [10], in which $\rho = 2035.42$ nm $^{-3}$ and $\eta = 4.70 \times 10^{-4}$ kg/m·s with same m and T but $\sigma_1 = 0$, in the present study with $\rho = 100$ nm $^{-3}$ and $\sigma_1 = 0.2$ nm, the evaluation of ζ_m is very different from the mesoscopic MD study, where ζ_m is very high and ζ_h is dominant in the evaluation of ζ_t .

Finally we plot $\zeta D/k_B T$ as a function of σ_2 in Fig. 4. These value first decreases as σ_2 increases, and then levels off at a σ_2 independent value of 0.79. This leveling-off takes place for σ_2 between 1 nm and 2 nm. $1/D_{MD}$ and $1/D_{SE}$ versus σ_2/σ_1 are essentially linear as seen in Fig. 2 and $D_{MD}/D_{SE} \approx 1.1$ for large values of σ_2/σ_1 as discussed above. Furthermore, ζ_h and ζ_{MD} versus σ_2 are also linear as seen in Fig. 4 and $\zeta_{MD}/\zeta_h \approx 0.115/0.159 = 0.72$ for large values of σ_2 . Multiplication of these two ratios gives the leveling-off value of $\zeta D/k_B T$. According to the Einstein relation, Eq. 3, however, the value of $\zeta D/k_B T$ is expected to be 1 for all σ_2 . If we choose the criterion that the solute can be considered as a Brownian particle as the diffusion coefficient of the solute obeys the Einstein relation between D and the lower bound of the size ratio above which the motion of the solute is Brownian is determined as $\sigma_2/\sigma_1 \approx 5$ since the value of $\zeta D/k_B T$ above this size ratio is independent on σ_2 , even though it is not exactly 1 as expected by the Einstein relation. This result is in accord with the earlier work of Ould-Kaddour and Levesque that for $M/m = 1$, the crossover to the hydrodynamics regimes is found to occur when $\sigma_2/\sigma_1 \sim 4$.[4]

For the case of $\sigma_2/\sigma_1 = 0.1$, the tracer behaves essentially as a point-like particle in the external potential created by the solvent molecules. The value of $\zeta D/k_B T$ at $\sigma_2/\sigma_1 = 0.1$ is 2.54 which is much larger than the leveling-off value of 0.79. The friction coefficient, $\zeta_{MD} = 0.040$ kg/mol·ps, from our MD simulation at $\sigma_2/\sigma_1 = 0.1$ is twice the hydrodynamic estimate of the friction by the Stokes formula, Eq. 2, $\zeta_h = 4\pi\eta r_2 = 0.019$ kg/mol·ps, but as the size ratio increases, they are almost equal at $\sigma_2/\sigma_1 = 0.5$ and for $\sigma_2/\sigma_1 \geq 1$ the deviation from the prediction by the Stokes formula becomes larger as discussed above. The diffusion coefficient, $D_{MD} = 21.3 \times 10^{-5}$ cm 2 /s, from our MD simulation at $\sigma_2/\sigma_1 = 0.1$ is slightly larger than the prediction from the Stokes–Einstein (SE) Eq. 1, $D_{SE} = 17.5 \times 10^{-5}$ cm 2 /s. While for higher values of σ_2/σ_1 , $D_{MD}/D_{SE} \approx 1.1$ and $\zeta_{MD}/\zeta_h \approx 0.72$, at $\sigma_2/\sigma_1 = 0.1$, $D_{MD}/D_{SE} \approx 1.2$ and $\zeta_{MD}/\zeta_h \approx 2.1$. The large value of $\zeta D/k_B T$ at $\sigma_2/\sigma_1 = 0.1$ compared to the leveling-off value is apparently due to the large value of ζ_{MD} . This indicates that the small tracer with equal mass of the solvent molecule can move easily around the gaps between large solvent molecules interacting through a repulsive LJ force each other, but in the calculation of the friction, the infinite mass of the point-like particle might cause it to feel an abnormally large friction in the external potential created by the solvent molecules.

5 Conclusion

In this paper we have presented a detailed investigation of the diffusion and friction of a Lennard–Jones tracer in

a solvent of similar molecules using microcanonical molecular dynamics (MD) simulations. This work was motivated by the determination of the lower bounds of the size and mass ratios above which the motion of the solute is Brownian. The criterion chosen to locate these bounds is that the diffusion coefficient of the solute obeys the Einstein relation between D and ζ . We did not, however, attempt an investigation for the lower bound of the mass ratio, since the only way to have a non-zero value for the friction coefficient is by first taking $M \rightarrow \infty$ according to the ergodic postulate of equilibrium statistical mechanics [20–22]. In the MD simulations we observed that D decreases with increasing M/m for lower ratios of M/m and the hydrodynamics limit, i.e., mass independent behavior, is reached for M/m above 5. The behavior of $1/D$ versus σ_2/σ_1 is essentially linear for σ_2/σ_1 higher than 2 and that of $1/D_{SE}$ predicted from the Stokes–Einstein relation with the slip boundary condition is also linear but for all the range of σ_2/σ_1 , D_{SE} slightly underestimates the diffusion coefficient of the tracer. We found that in the estimation of the friction coefficient ζ of the tracer, ζ can be determined correctly from the time dependent friction coefficient by measuring the extrapolation of its long time to $t = 0$, but it is difficult to determine ζ from the slope of the time dependent coefficient due to the scaling of the slope as $1/N$ and from the decay rate of the momentum autocorrelation function due to the fast decay of the correlation function. It is also found that the friction coefficient of the tracer varies linearly with σ_2 in accord with the prediction of the Stokes formula but shows a smaller slope than the Stokes prediction. The value of $\zeta D/k_B T$ as a test of the Einstein relation first decreases as σ_2 increases, and then levels off at a σ_2 independent value. This leveling-off takes place for σ_2 between 1 nm and 2 nm. For the values of σ_2/σ_1 higher than 5 approximately, the behavior of the friction and diffusion coefficients is well described by the Einstein relation, from which the tracer is considered as a Brownian particle.

Acknowledgments This research was supported by Kyungsung University Research Grants in 2010.

References

1. Landau LD, Lifshitz EM (1963) Fluid Mechanics. Pergamon, London
2. Phillips GD (1981) J Phys Chem 85:2838–2843
3. Forster D (1975) Hydrodynamics Fluctuations, Broken Symmetry, and Correlation Functions. Benjamin, Reading, MA
4. Ould-Kaddour F, Levesque D (2001) Phys Rev E 63:011205(9)
5. Willeke M (2003) Mol Phys 101:1123–1130
6. Sokolovskii RO, Thachuk M, Patey GN (2006) J Chem Phys 125:204502(10)
7. Cappelezzo M, Capellari CA, Pezzin SH, Coelho LAF (2007) J Chem Phys 126:224516(5)
8. Funazukuri T, Kong CY, Kagei S (2008) J Supercritical Fluids 46:280–284
9. Harris KR (2009) J Chem Phys 131:054503(8)
10. Lee SH, Kapral R (2004) J Chem Phys 121:11163–11169
11. Malevanets A, Kapral R (1999) J Chem Phys 110:8605–8613
12. Malevanets A, Kapral R (2000) J Chem Phys 112:7260–7269
13. Malevanets A, Kapral R (2004) Lect Notes Phys 640:116–149
14. Weeks JD, Chandler D, Andersen HC (1971) J Chem Phys 54:5237–5247
15. Meier M, Laesecke A, Kabelac S (2004) J Chem Phys 121:3671–3687; ibid (2004) ibid 121:9526–9535; ibid (2005) ibid 122:014513(9)
16. Allen MP, Tildesley DJ (1987) Computer Simulation of Liquids. Oxford Univ Press, Oxford
17. Swope WC, Andersen HC, Berens PH, Wilson KR (1982) J Chem Phys 76:637–649
18. Lee SH (2007) Bull Korean Chem Soc 28:1371–1374
19. Españo P, Zúñiga I (1993) J Chem Phys 98:574–580
20. Kubo R (1957) J Phys Soc Jpn 12:570–586
21. Kubo R (1966) Rep Prog Phys 29:255–284
22. Kubo R (1969) In: Parry WE et al. (eds) Many-body problems, the fluctuation-dissipation theorem. Benjamin, New York
23. Ould-Kaddour F, Levesque D (2003) J Chem Phys 118:7888–7891
24. Ryckaert JP, Ciccotti G, Berendsen HJC (1977) J Comput Phys 23:327–341
25. Lee SH (2010) Bull Korean Chem Soc 31:959–964
26. Hynes JT, Kapral R, Weinberg M (1979) J Chem Phys 70:1456–1466